Impact of Central ECCD on Steady-State Hybrid Scenario in DIII-D

C.C. Petty,[1,a] R. Nazikian,[2] M.A. Van Zeeland,[1] D.C. Pace,[1] B.A. Grierson,[2] Xi Chen,[1] E. Kolemen,[3] G.R. McKee,[4] R. Prater[1] and F. Turco[5]

[1]*General Atomics, P.O. Box 85608, San Diego, CA, USA*
[2]*Princeton Plasma Physics Laboratory, Princeton, NJ, USA*
[3]*Princeton University, Princeton, NJ, USA*
[4]*University of Wisconsin - Madison, Madison, WI, USA*
[5]*Columbia University, New York, NY, USA*

[a)]Corresponding author: petty@fusion.gat.com

Abstract. "Steady-state" hybrid plasmas in DIII-D with zero surface loop voltage have been maintained for up to two current relaxation times using 3.4 MW of central electron cyclotron current drive (ECCD). In addition to driving ≈0.2 MA of plasma current, central ECCD leads to significant changes in Alfvén eigenmode (AE) activity and thermal transport. For neutral-beam-only heating, strong AE activity is observed that causes a ~35% degradation in the neutron rate. With central ECCD this AE activity is suppressed, replaced by a bursty energetic particle mode that appears more benign as the neutron rate is closer to the classical value. The electron thermal diffusivity increases by ≈50% for 2.4 MW of ECCD compared to neutral-beam-only cases. Fortunately, the global thermal confinement factor remains the same (H_{98y2}=1.4) as the higher thermal transport for P_{EC}=2.4 MW hybrids is offset by the decreased fast ion transport resulting from AE suppression.

INTRODUCTION

Experiments in the DIII-D tokamak have been developing a "steady-state" hybrid scenario using a mixture of central electron cyclotron current drive (ECCD), neutral beam current drive and bootstrap current to achieve zero surface loop voltage for ≤2 current relaxation times [1]. Central ECCD plays a vital role in this steady-state scenario, driving ≈0.2 MA out of ≈1.0 MA plasma current using 3.4 MW of injected power, as shown in figure 1. Concurrent with the application of central ECCD, significant changes in Alfvén eigenmode (AE) activity and thermal transport are observed. Fully non-inductive hybrids have been created in DIII-D with and without ELM suppression using n=3 resonant magnetic perturbations; the impact of central ECCD is similar in either case (this paper mainly discusses ELM suppression cases).

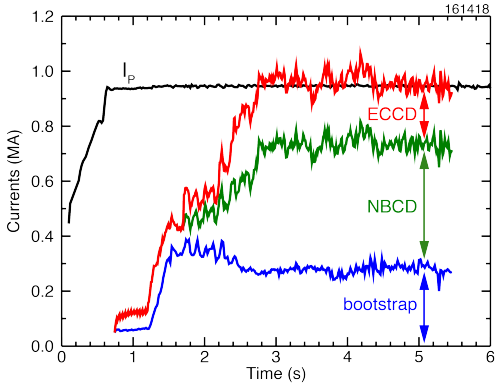

FIGURE 1. Modeled non-inductive currents for a steady-state hybrid plasma in DIII-D.

An important feature of the hybrid regime in DIII-D is the anomalously broad current profile. In the absence of ECCD, neutral-beam-heated hybrid plasmas do not develop sawteeth since q_{min} is maintained above 1 by anomalous poloidal magnetic flux pumping [2,3]. However, the addition of localized ECCD (with calculated peak magnitudes as high as ~8 MA/m^2) causes sawteeth to appear, indicating that the intense ECCD overwhelms the flux pumping mechanism. Interestingly, spreading out the ECCD

Radio Frequency Power in Plasmas
AIP Conf. Proc. 1689, 090002-1–090002-4; doi: 10.1063/1.4936539

deposition to reduce the peak current density by a factor of two-to-four lessens or even eliminates the sawteeth activity without negatively impacting the current drive efficiency.

SUPPRESSION OF ALFVÉN EIGENMODES

High-beta hybrids with central ECCD exhibit much weaker core MHD than similar plasmas without ECCD. Figure 2(a) shows the cross-amplitude spectrum from the CO_2 interferometer for a hybrid plasma with neutral-beam-only heating (and ≈0.01 V surface loop voltage). In additional to the low frequency neoclassical tearing modes (NTM) that are ubiquitous in the DIII-D hybrid regime, a large number (8-10) of Alfvén eigenmodes (AE) are observed at high frequencies (100-250 kHz). The calculated Alfvén gap structure indicates these excited modes are in the TAE/EAE frequency range. During ECCD, this high frequency AE activity is suppressed, as seen in figure 2(b), replaced by a bursty energetic particle mode with toroidal mode numbers n=1-5 that rapidly chirps down in frequency. This intermittent mode during ECCD is fishbone-like but has a dominant n=2 sideband that strongly couples to the m/n=3/2 NTM.

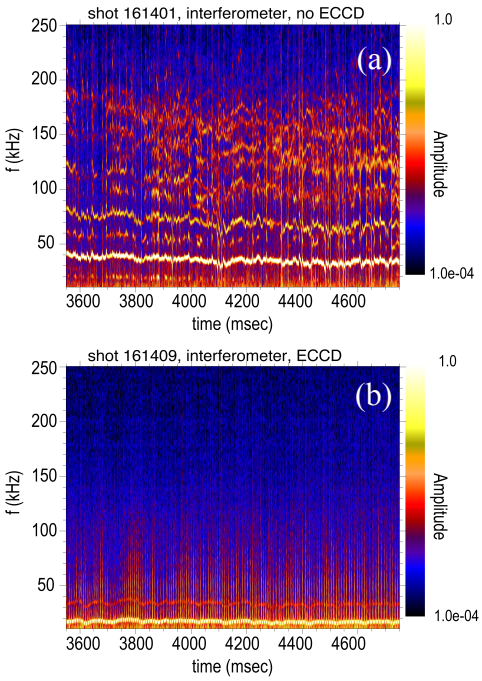

FIGURE 2. Cross-amplitude spectrum from CO_2 interferometer for hybrids with (a) only neutral beams, and (b) ECCD and neutral beams.

For hybrid plasmas with neutral-beam-only heating and strong AE activity, large beam ion transport is needed in TRANSP to match the experimental neutron rate. Figure 3(c) shows that the calculated neutron rate from TRANSP without anomalous beam ion diffusion (red curve) is well above the measured neutron rate (blue curve) for hybrids without ECCD. In order to match the experimental neutron rate, TRANSP requires a beam ion diffusion coefficient of ~1 m^2/s [figure 3(d)]. The anomalous beam ion transport increases with time in correlation with higher TAE/EAE activity, as measured by the CO_2 interferometer in the 50-400 kHz band. For a similar steady-state hybrid plasma with central ECCD, the experimental neutron rate is closer to the classical value [figure 3(g)] and the implied beam ion transport coefficient is less than half the neutral-beam-only case [figure 3(h)]. Therefore, the fishbone-like mode observed in hybrids with central ECCD is apparently more benign than the AEs in regard to anomalous beam ion transport.

INCREASE IN THERMAL TRANSPORT

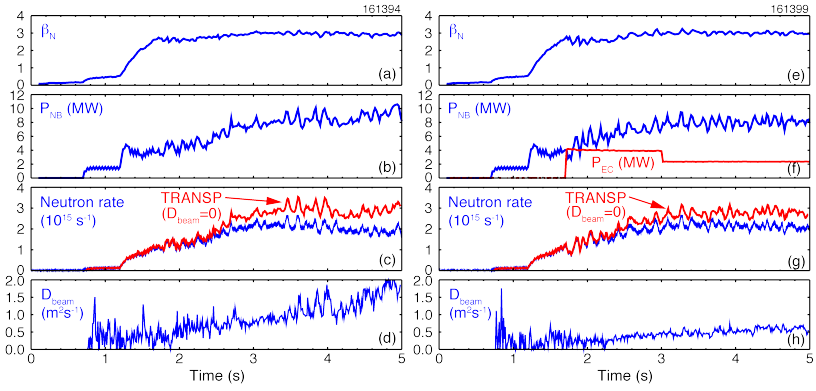

FIGURE 3. Anomalous beam ion diffusion coefficient needed by TRANSP to match experimental neutron rate for hybrids with (a)-(d) only neutral beams, and (e)-(h) ECCD and neutral beams.

Central electron heating during ECCD has a significant effect on all plasma profiles in steady-state hybrid plasmas. As seen in figure 4, the internal transport barrier (ITB) evident in neutral-beam-only hybrids, especially in the ion temperature and toroidal rotation, is not present in hybrids with ECCD. While central ECCD is effective at bringing the electron and ion temperatures closer together, above P_{EC}=2.3 MW the changes in the plasma profiles seem to saturate.

The thermal diffusivities increase systematically with higher central electron heating from ECCD, while the momentum diffusivity varies less and the electron particle diffusivity does not change systematically. Transport analysis from the TRANSP code is shown in figure 5 using a value of D_{beam} that best matches the experimental neutral rate as a function of time for each discharge. Both χ_e and χ_i increase across the plasma radius (except near the axis) with higher ECCD power. Since $\chi_e \approx \chi_i$, using equal amounts of electron and ion heating will naturally give $T_e \approx T_i$ in these plasmas. As seen in figure 5(c), the D_{elec} profile flattens during ECCD (increasing in the core and decreasing in the edge), which causes the plasma density profile to broaden. Finally, χ_{mom} increases some during ECCD but not as much as χ_e and χ_i.

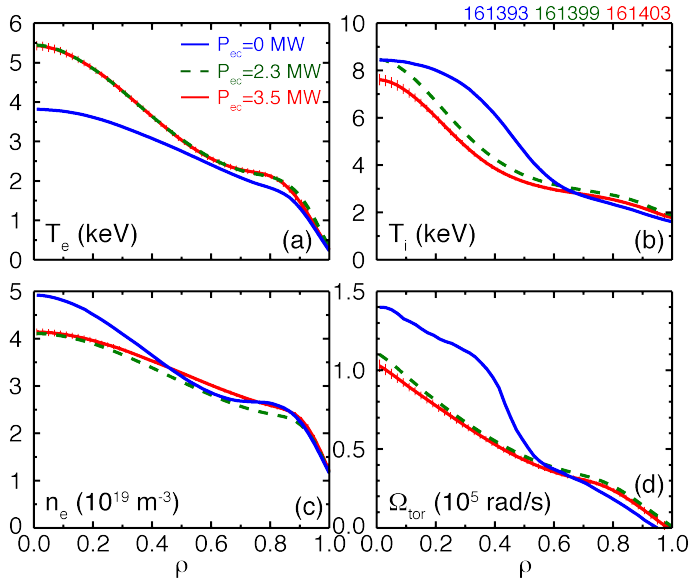

FIGURE 4. Plasma profiles for different ECCD powers: (a) electron temperature, (b) ion temperature, (c) density and (d) toroidal rotation.

A time dependent transport analysis shows that the electron and ion thermal transport jump higher in response to central electron heating. Figure 6 plots the time history of χ_e, χ_i and D_{elec} at ρ=0.5 for three hybrids with different amounts of central ECCD. Compared to a neutral-beam-only case (blue curves), the electron thermal diffusivity increases by ≈50% for 2.4 MW (green curves) and ≈100% for 3.4 MW of ECCD (red curves). The increase in ion thermal diffusivity during central electron heating is more dramatic, but this is because $\chi_i << \chi_e$ for the neutral-beam-only case while $\chi_i \approx \chi_e$ during ECCD. Compared to the thermal diffusivities, the electron particle diffusivity has a weak dependence on P_{EC} in figure 6(d), but this is a consequence of plotting D_{elec} at ρ=0.5 which is a pivot point in the flattening of the D_{elec} profile during ECCD [see figure 5(c)]. The transport coefficients plotted in figure 6 from TRANSP take into account the time varying neutral beam ion transport; if this is not done then the transport coefficients would appear to increase steadily with time instead of being nearly constant (except when the ECCD power changes). Beam ion transport from MHD activity is also the main reason why global thermal confinement decreases over time in these hybrids. The H_{98y2} factor calculated in the normal way slowly decreases during the discharge, but after correcting for the increase in fast ion transport the H_{98y2} factor becomes fairly constant over time. Beam ion transport lowers H_{98y2} since it reduces the neutral beam heating effectiveness.

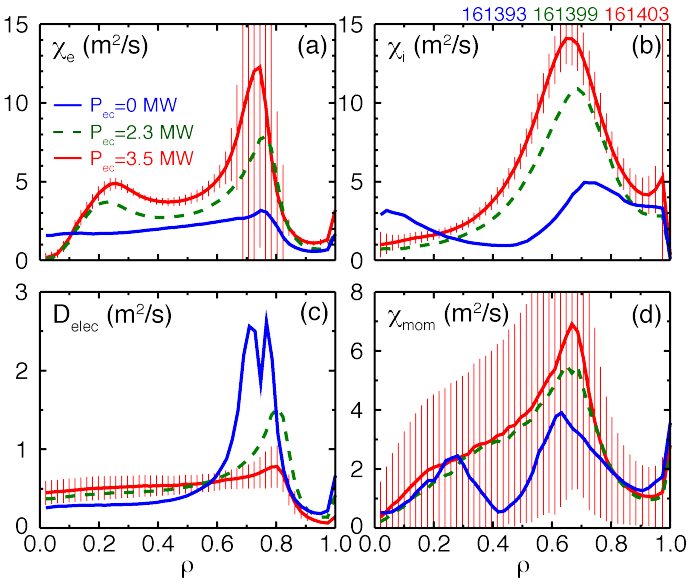

FIGURE 5. TRANSP diffusivity profiles for different ECCD powers: (a) electron thermal, (b) ion thermal, (c) particle and (d) momentum.

An important feature of these steady-state hybrid plasmas is that the global thermal confinement factor remains the same (H_{98y2}=1.4) for the neutral-beam-only and P_{EC}=2.4 MW hybrids despite the large increase in the electron and ion thermal diffusivities for the latter case. The reason for this is that the higher thermal transport during ECCD is offset by the improved fast ion transport as the TAE/EAE modes are replaced by the more benign fishbone-like mode. These mitigating effects appear to explain why steady-state hybrid performance responds so positively to high power ECCD, whereas for many H-mode regimes the performance noticeably decreases with higher T_e/T_i [4]. However, for the P_{EC}=3.4 MW hybrids the higher thermal transport does cause a noticeable drop in confinement (H_{98y2}=1.2).

This material is based upon work supported by the U.S. Department of Energy, Office of Science, Office of Fusion Energy Sciences, using the DIII-D National Fusion Facility, a DOE Office of Science user facility, under Awards DE-FC02-04ER54698, DE-AC02-09CH11466, DE-FG02-08ER54999, and DE-FG02-04ER54761. DIII-D data shown in this paper can be obtained in digital format by following the links at https://fusion.gat.com/global/D3D_DMP.

REFERENCES

[1] F. Turco et al., Phys. Plasmas 22, 056113 (2015)
[2] M.R. Wade et al., Nucl. Fusion 45, 407 (2005)
[3] C.C. Petty et al., Phys. Rev. Lett. 102, 045005 (2009)
[4] C.C. Petty et al., Phys. Rev. Lett. 83, 3661 (1999)

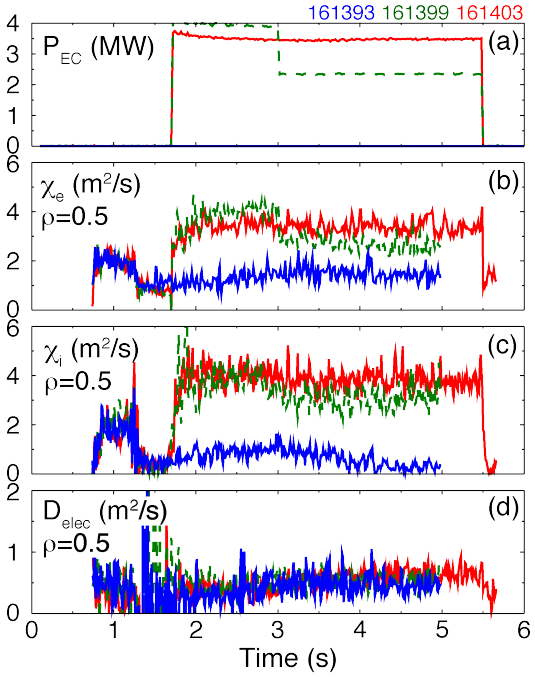

FIGURE 6. Time history of TRANSP diffusivities at ρ=0.5: (a) ECCD power, (b) electron thermal, (c) ion thermal, (d) particle.